Experimental study of oblique impact between dry spheres and liquid layers

Jiliang Ma,* Daoyin Liu,† and Xiaoping Chen‡
Key Laboratory of Energy Thermal Conversion and Control of Ministry of Education, School of Energy and Environment, Southeast University, Nanjing 210096, China

(Received 9 June 2013; revised manuscript received 6 August 2013; published 24 September 2013)

Liquid addition is common in industrial fluidization-based processes. A detailed understanding of collision mechanics of particles with liquid layers is helpful to optimize these processes. The normal impact with liquid has been studied extensively; however, the studies on oblique impact with liquid are scarce. In this work, experiments are conducted to trace Al_2O_3 spheres obliquely impacting on a surface covered by liquid layers, in which the free-fall spheres are disturbed initially by a horizontal gas flow. The oblique impact exhibits different rebound behaviors from normal collision due to the occurrence of strong rotation. The normal and tangential restitution coefficients (e_n and e_t) and liquid bridge rupture time (t_{rup}) are analyzed. With increase in liquid layer thickness and viscosity, e_n and e_t decline, and t_{rup} increases. With increase in tangential velocity, e_t decreases first and then increases, whereas e_n remains nearly unchanged, and t_{rup} decreases constantly. A modified Stokes number is proposed to further explore the relation between restitution coefficients and the impact parameters. Finally, an analysis of energy dissipation shows that the contact deformation and liquid phase are the two main sources of total energy dissipation. Unexpectedly, the dissipative energy caused by the liquid phase is independent of tangential velocity.

DOI: 10.1103/PhysRevE.88.033018 PACS number(s): 47.55.Kf, 45.70.−n, 45.50.Tn, 47.55.nk

I. INTRODUCTION

In many industrial fluidization-based processes, such as pharmacy, granulation, and agriculture, particles are usually coated with liquid layers. When interacting with each other or colliding with a wall, the wet particles impact and rebound differently from dry particles. This is largely due to the formation of a liquid bridge which causes the particles to exhibit different flow behaviors when compared with dry systems. Manipulation of these flows requires a detailed understanding of the individual collision mechanics with the presence of a liquid bridge.

Regarding the general individual collision, three different situations can be identified: (a) collision between spheres, (b) collision between spheres fully immersed in liquid, and (c) collision between spheres covered with liquid layers. For brevity, in the following they are denoted as (a) dry impact, (b) immersed impact, and (c) liquid bridged impact, respectively.

Dry impact. The classical approach to the characterization of particle impact and rebound behaviors is associated with the restitution coefficient [1] which is defined as the ratio between rebound and impact velocities of particles. Based on that, many theories for normal impact (e.g., elastic [2–4], elastic-plastic [5], and viscoelastic impact [6,7]) have been developed. When concerning oblique impact, rebound behaviors can be distinguished as rolling and sliding regimes according to different tangential velocity. Maw *et al*. [2,8] demonstrated the need to consider tangential compliance in the rolling regime and introduced the tangential restitution coefficient to characterize the oblique impact. It was then confirmed by Thornton and Yin [4] through numerical simulation. Kharaz *et al*. [9] extended Maw's theory to characterize the oblique impact in terms of normal and tangential restitution coefficient as well as coefficient of friction. The effects of moisture content in particles on the impact characteristics have also been the subject of important work. The normal restitution coefficient was found to decrease significantly with increasing moisture content [10,11] and increase first to a maximum value, and then decrease with increasing impact velocity [12].

Immersed impact. The collision mechanics of particles in the viscous liquid have been studied extensively for its omnipresence in the liquid-solid flows. Lundberg and Shen [13] found that the rebound behavior of the spheres placed in a fluid depends heavily on the liquid viscosity. Davis *et al*. [14] investigated the dynamic deformation of a solid elastic sphere which is immersed in a viscous liquid when making head-on impact on a plate; they established a rational criterion (Stokes number, $\mathrm{St} = mV_i/6\pi\mu a^2$, where m is the mass of sphere, a is its radius, V_i is the initial impact velocity, and μ is the liquid viscosity) to predict whether a sphere would rebound subsequent to impact. According to Davis *et al*. [14], when $\mathrm{St} < \mathrm{St}_c$, where St_c is the critical Stokes number, the sphere sticks to the plate surface. Based on the same definition of St, Gondret *et al*. [15] found that the restitution coefficient increases rapidly for $\mathrm{St} > \mathrm{St}_c$ and approaches an asymptotic value for $\mathrm{St} > \mathrm{St}_c$. Similar results have also been obtained by Joseph *et al*. [16,17], Zenit and Hunt [18] and Stocchino and Guala [19].

Liquid bridged impact. Impact characteristics on a liquid layer have drawn great attention in the past decades due to the ubiquity in industry. However, liquid bridged impact is more complex than "dry impact" and "immersed impact" due to the formation of a liquid bridge. Barnocky and Davis [20] dropped small spheres upon a plate covered with a viscous liquid layer and first observed the existence of critical drop height, above which rebound occurs. This theory was subsequently extended by Matthewson [21] who pointed out that the impulse required for a sphere to separate from the liquid layer strongly depends on the sphere diameter, liquid viscosity, and layer

*topony@163.com
†Corresponding author: dyliu@seu.edu.cn
‡xpchen@seu.edu.cn

thickness. Davis *et al*. [22] found that the restitution coefficient increases with $\mathrm{St}/\mathrm{St}_c$. Kantak *et al*. [23] further proposed a simple model, $e_{\mathrm{wet}} = e_{\mathrm{dry}}(1 - \mathrm{St}_c/\mathrm{St})$ (where e_{wet} and e_{dry} are restitution coefficients obtained for wet and dry impact, respectively), to predict the restitution coefficient. Antonyuk *et al*. [24] demonstrated that the energy loss caused by the viscous damping force and drag force are more significant than other factors in the energy dissipation process. Recently, the Hrenya group from Colorado University has undertaken much work to characterize the collision mechanics in the presence of liquid: Donahue *et al*. [25,26] developed a scaling theory to characterize the three-body collision that considers liquid bridge force existing between agglomerating particles initially and pressure dependence in the liquid viscosity. In another paper, they explored particle-particle oblique collisions and observed a rotating doublet for two obliquely colliding particles before deagglomeration. Based on the results, they introduced a dimensionless centrifugal number ($\mathrm{Ce} = m\omega_r^2/\sigma$, where ω_r is angular velocity and σ is the surface tension of liquid) together with the Stokes number ($\mathrm{St} = mV_i/6\pi\mu a^2$) to characterize the regime map of outcomes for oblique collision between two particles [27]. Kantak and Davis [28] studied the rebound behavior of spheres obliquely impacting on a wetted surface and found that the tangential rebound velocity is reduced only by a small amount, while the normal rebound velocity is reduced substantially by viscous losses.

All of the above work in the area of collisions in the presence of liquid layer, except that of Kantak and Davis [28], has been limited to head-on impact, while the effects of liquid layers on oblique impacts are relatively unstudied. This is largely due to the difficulties in the introduction of tangential velocity into the oblique impact experiment. The existing methods are based on free-fall spheres impacting on an inclined plate. It implies that the liquid employed must be highly viscous and thin enough to avoid uneven distribution due to the gravity induced flow. Moreover, the inclined angle must be limited to a small value, resulting in a narrow range of tangential velocities of spheres. Consequently, to date, a continuum description for the rebound behavior of spheres obliquely impacting on a liquid layer that covers a wide range of viscosities and thickness is still far from established.

This paper proposes an experimental program for the oblique impact between spheres and a wet plate, viz., disturbing the free-fall spheres by introducing a horizontal gas flow to make it fall obliquely. Impact dynamics are investigated as a function of tangential impact velocity and liquid properties. The mechanics of oblique impact between spheres and liquid layers are highlighted. From this, the theory of Stokes number and energy dissipation analysis are also used to analyze the collision dynamics.

II. EXPERIMENT

A. Experimental setup

Figures 1 and 2 show the diagram and digital image of the experimental system, respectively. A stainless steel plate of thickness 20 mm, length 450 mm, and width 130 mm, held by a wooden slot, was employed as the target. The levelness of the target was maintained by four adjustable legs mounted at its bottom; a nozzle that provides horizontal gas flow was fixed on the left side of the unit located 300 mm above the target. Another nozzle is held at a predetermined height 320 mm above the target and connected to a vacuum pump. A high-speed video camera (FASTCAM SA4) with resolution of 1024×1024 pixels and 2000 frames per second was put 0.5 m away from the object plate to record the movement of spheres; two 800-W lamps were positioned symmetrically on both sides of the target to get the optimal illumination conditions. Behind the apparatus, there is a piece of black cloth to act as background.

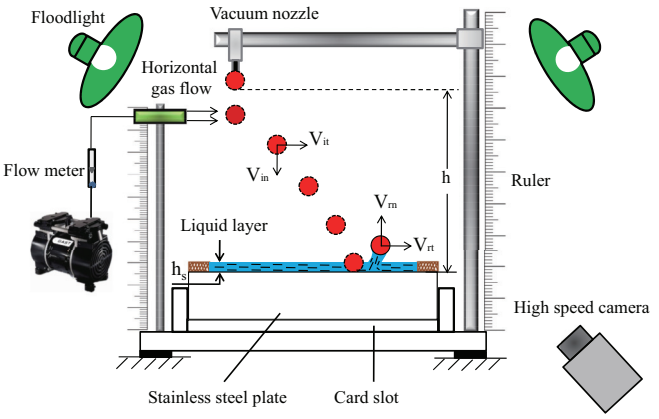

FIG. 1. (Color online) Schematic diagram of the experimental system.

B. Materials

The spheres used are 6-mm elastic-plastic Al_2O_3 particles with density of 2000 $\mathrm{kg/m^3}$. The distilled water and aqueous solutions of hydroxypropyl methylcellulose (HPMC) were employed as the liquid layer with different concentrations for variation of viscosity. Dynamic viscosities of HPMC solutions were measured using a revolving viscometer (NXS-4) and ranged from 1 mPa s for clear water, up to 32.1 mPa s for an 8% aqueous solution of HPMC at a temperature of about 30 °C. The thickness of the liquid layer was determined as the ratio of the liquid volume to the plate area.

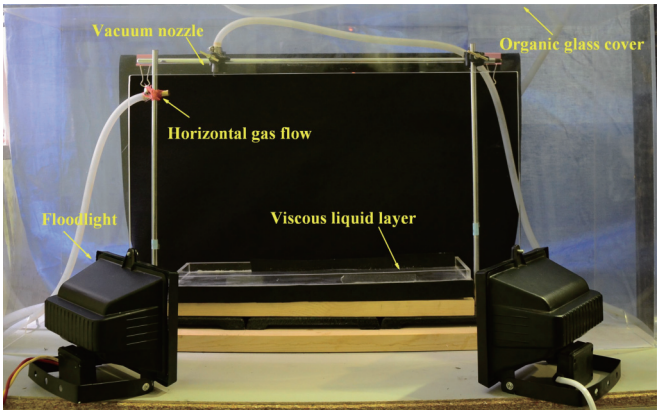

FIG. 2. (Color online) Photograph of experimental setup.

C. Experimental procedure

The viscous liquid is first sprayed onto the plate and uniformly distributed on the surface with the aid of a brush. An Al_2O_3 sphere was held to the vacuum nozzle and released without initial velocity or rotation by switching off the vacuum pump. Then we injected a horizontal N_2 gas flow to disturb the free-fall sphere and make it move obliquely. By adjusting the flow rate of the N_2 gas, different tangential velocities of spheres can be determined. The pre- and postimpact images were captured by the high-speed video camera.

D. Experimental data processing

The images were subsequently analyzed to determine the sphere centroids using self-programmed software on the basis of MATLAB. The velocity of the sphere along its whole trajectory can be evaluated, starting from the discrete sampled position using a first-order backward differencing scheme, based on which, normal and tangential restitution coefficients (e_n and e_t) were obtained. Each test condition was repeated for at least five times to get the representative results.

Concerning the impact on a liquid layer, a significant contribution to the energy dissipation is the liquid bridge force arising during the rebound. Therefore, in order to characterize the effects of the liquid, the restitution coefficients should be defined as a ratio of the sphere velocity at the bridge rupture to the velocity at the contact with the liquid before impact.

$$e_n = \frac{V_{\mathrm{nr}}}{V_{\mathrm{ni}}}, \quad e_t = \frac{V_{\mathrm{tr}}}{V_{\mathrm{ti}}}, \tag{1}$$

where V_{ni} and V_{ti} are the normal and tangential impact velocities of the spheres (m/s); V_{nr} and V_{tr} are corresponding rebound velocities at the bridge rupture (m/s).

The restitution coefficients also represent the energy dissipation in the impact and rebound process.

$$e_n = \sqrt{1 - \frac{E_{\mathrm{diss}\text{-}n}}{E_{\mathrm{in}}}}, \tag{2}$$

$$e_t = \sqrt{1 - \frac{E_{\mathrm{diss}\text{-}t}}{E_{\mathrm{it}}}}. \tag{3}$$

$E_{\mathrm{diss}\text{-}n}$ and $E_{\mathrm{diss}\text{-}t}$ represent normal and tangential energy loss; E_{in} and E_{it} are defined as initial kinetic energy in the normal and tangential direction.

III. RESULTS

Figure 3 plots the height of the sphere during normal impact on dry and wetted plates. Figure 4 shows the velocity of the sphere versus its trajectory for wet and dry impact. It can be seen that both peak height and rebound velocity for the wet case are much smaller than the dry condition. Moreover, the rebound velocity decreases more sharply when the liquid bridge is present. These results indicate the important role that the liquid layer plays in the total energy dissipation for wet impact. Besides that, the effects of liquid bridge force on the energy dissipation process should not be neglected either.

Figure 5 provides examples of sphere trajectories for oblique impact on a plate with and without a liquid layer, through which the peak height of rebound trajectories can be estimated. Similar to the normal impact, the peak height for oblique impact in the wet case is much smaller than that of the dry case. Figure 6, plotting the tangential and normal velocities of pre- and postimpact for oblique impact on a water layer, shows that the presence of a liquid layer reduces a large amount of normal velocities but a small fraction of tangential component.

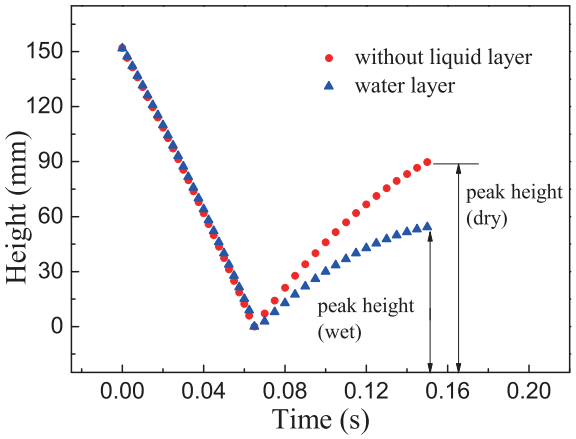

FIG. 3. (Color online) Variation of sphere height for normal impact; (red circles) without liquid layer; (blue triangles) with water layer; layer thickness: 1 mm.

A. Rotation after impact

The whole impact process of spheres on a plate covered with a liquid layer can be divided into five subprocesses: contact, immersion, bridge formation, bridge extension, and bridge rupture. A close view of the colliding event as shown in Fig. 7 reveals that the oblique impact exhibits significantly different rebound behaviors in comparison to the normal impact. Rotation arises after oblique impact, which changes the shape of the liquid bridge and the corresponding liquid bridge force, ultimately affecting the sphere velocity.

In order to explore the origin of rotation arising after oblique impact, a separate set of experiments was carried out. In these

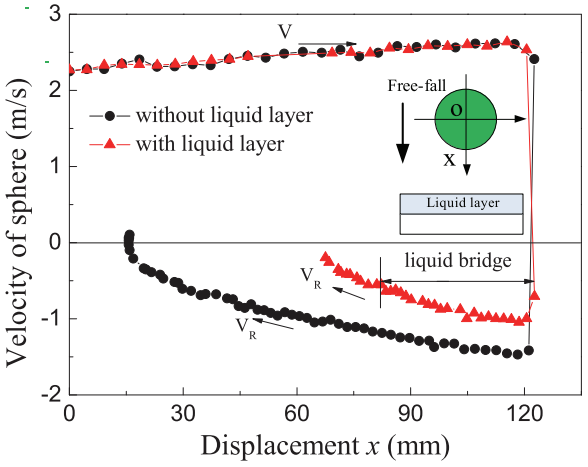

FIG. 4. (Color online) Velocity-displacement curve for normal impact.

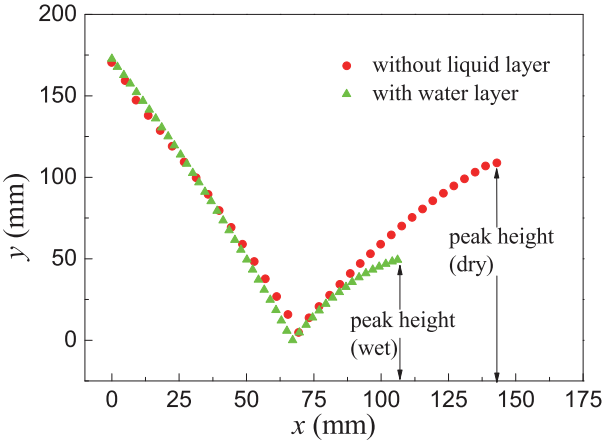

FIG. 5. (Color online) Sphere trajectories during oblique impact for dry and wet condition; (red circles) without liquid layer, $V_{ni} = 2.51$ m/s, $V_{ti} = 0.90$ m/s; (green triangles) with water layer, $V_{ni} = 2.51$ m/s, $V_{ti} = 0.90$ m/s, layer thickness: 1 mm.

tests, the spheres were marked with stripes to determine the rotation and set to obliquely impact on a dry plate. The sampled pictures for pre- and postimpact are provided in Fig. 8. It can be seen that no rotation was observed until the sphere contacts the plate surface, which indicates the role of sphere-plate contact in subjecting a torque to the sphere surface that induces rotation.

Though rolling during contact is the main cause of rotations, it is not the only factor that controls the angular velocity. The viscous and drag forces caused by the liquid layer may also influence the rotation of spheres. Therefore, it is necessary to obtain the key factors that determine the rotation of rebound spheres. The dependence of angular velocities on the tangential impact velocity and various liquid layer thicknesses is plotted in Fig. 9. Meanwhile, in the same plot are reported the experimental data from Kharaz *et al.* [9,29], which were obtained under dry impact tests that used materials and apparatus similar to that used in the present study. As can be seen, the angular velocity increases with tangential velocity and decreases with the increasing of liquid layer thickness. The comparison also reveals that the angular velocity for

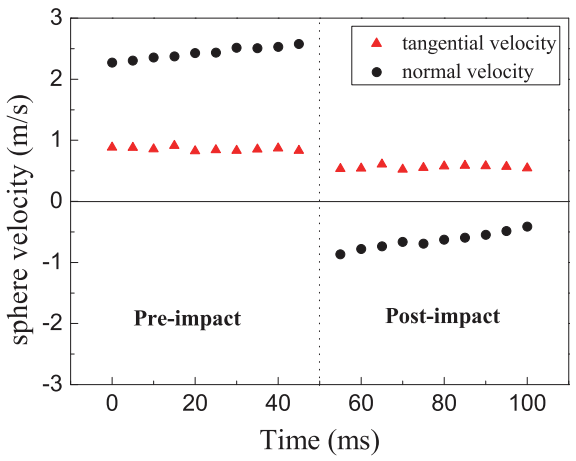

FIG. 6. (Color online) Variation of normal and tangential velocities with time for oblique impact on water layer (layer thickness: 1 mm).

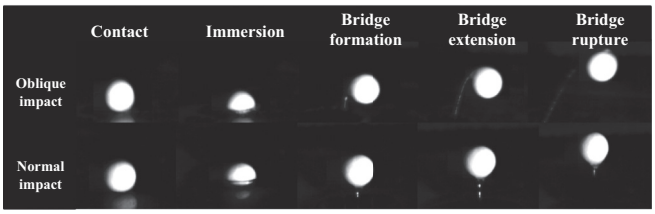

FIG. 7. Colliding events for oblique and normal impact.

the dry impact is always higher than that of the wet case, which indicates that the presence of liquid inhibits the rotation of spheres, due to the torque imposed by the viscous force that acts in the direction opposite to the rotation. But as the tangential velocity increases, the differences between the dry and wet case in the angular velocity are shortened, implying that the inhibition effects from liquid are gradually weakened with increasing tangential velocity. Note that the effect of layer thickness on the angular velocity can be nearly neglected until the tangential velocity exceeds a critical value of 0.78 m/s, according to which, we proposed an assumption that the tangential velocity is the key factor in the determination of rotation. In other words, layer thickness and viscosity have comparably weak effects on the angular velocity until the tangential velocity exceeds certain critical values. In order to confirm this hypothesis, we plotted the angular velocities obtained under different liquid layer thickness and viscosities versus tangential velocity in Fig. 10. It can be seen that a critical tangential velocity (also referred to as V_{tc}) exists, below which the angular velocities under various layer thicknesses are nearly the same. When the tangential velocity is larger than V_{tc}, the data scatter, indicating that liquid properties play an important role in determining the angular velocities.

B. Effects of layer thickness

Figure 11 shows the effects of liquid layer thickness on e_t and e_n as well as liquid bridge rupture time (t_{rup}). The increasing of liquid layer thickness causes declines of e_t and e_n and an increase of t_{rup}. Moreover, e_n is always smaller than e_t in the case of the same layer thickness, which agrees well with the experimental results obtained by Kantak and Davis [28].

Since the restitution coefficient is related to the fraction of kinetic energy retained after the impact, the declines of e_n and e_t indicate that the energy loss caused by the liquid layer is dramatically enhanced by the increasing of layer thickness.

For the case that a sphere impacts on two layers with different thickness (h_1, h_2; $h_1 > h_2$), the corresponding energy loss E_1 is always larger than E_2 owing to an additional dissipative process arising during the distance of $h_1 - h_2$. That is the reason that e_n decreases with the increasing liquid layer thickness.

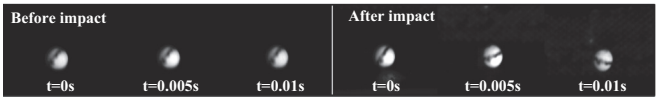

FIG. 8. Rotation of sphere before and after impact.

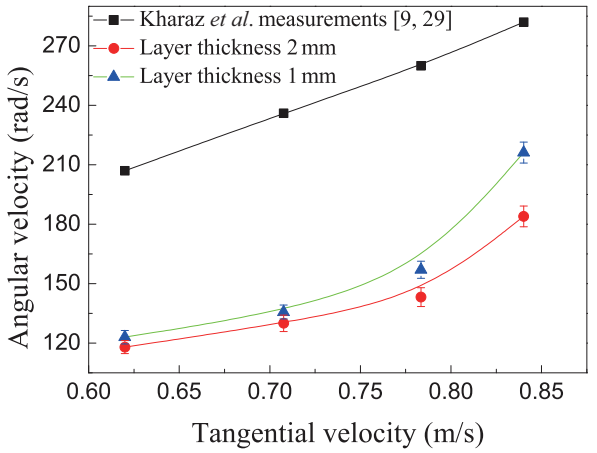

FIG. 9. (Color online) Effect of tangential velocity on angular velocity; liquid viscosity: 20.3 mPa s.

The drag force exerting on the tangential moving sphere can be calculated by the following equation:

$$F_D = \tfrac{1}{2} C_D A \rho U^2, \tag{4}$$

where C_D is the drag coefficient; A is the characteristic area; ρ is the density of liquid; U is the sphere velocity. For the present study, C_D and ρ remain constant. A increases with the liquid layer thickness so that F_D and the corresponding energy loss increase, thus decreasing e_t.

To the best of our knowledge, t_{rup} is proportional to the rupture energy (W_{rup}), and W_{rup} increases with the liquid bridge volume, V ($W_{\text{rup}} \sim V$) [30]. Concerning the present study, V increases with the layer thickness, causing an increase of W_{rup} and a growth of t_{rup}.

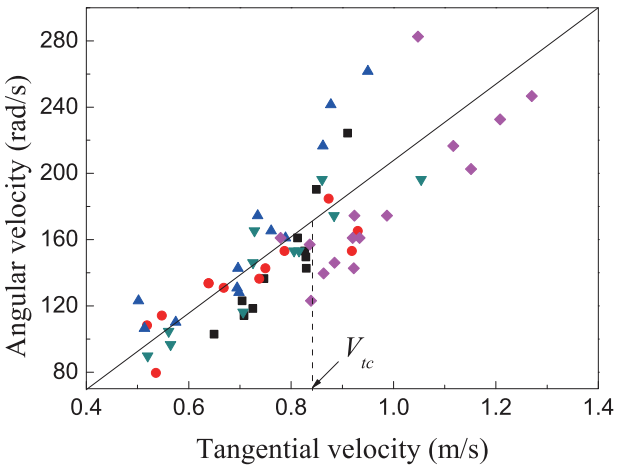

FIG. 10. (Color online) Angular velocities obtained for different layer thicknesses and liquid viscosities versus tangential impact velocity; (black squares) layer thickness: 1 mm; liquid viscosity: 20.3 mPa s; (red circles) layer thickness: 2 mm; liquid viscosity: 20.3 mPa s; (blue triangles) layer thickness: 1 mm; liquid viscosity: 1 mPa s; (green inverted triangles) layer thickness: 2 mm; liquid viscosity: 1 mPa s; (pink diamonds) layer thickness: 2 mm; liquid viscosity: 31.4 mPa s.

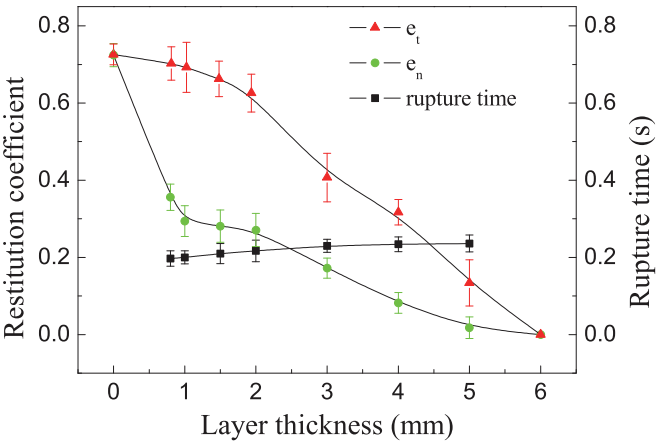

FIG. 11. (Color online) e_t, e_n, and t_{rup} versus layer thickness. (tangential velocity: 0.578 m/s; liquid viscosity: 20.3 mPa s).

C. Effects of liquid viscosity

Figure 12, plotting e_t, e_n, and t_{rup} as a function of liquid viscosity, shows that e_t and e_n decrease systematically with increasing of liquid viscosity. Moreover, they drop sharply when liquid viscosity exceeds 20 mPa s, which indicates that viscous damping dominates the energy dissipation process under high viscosity. t_{rup} increases with the liquid viscosity.

Concerning the present study, the normal energy dissipation is derived from the liquid viscous force F_{vis}. Thus the energy loss can be estimated as

$$E_{\text{diss-}n} = \int_0^h F_{\text{vis}} dx. \tag{5}$$

Adams and Edmondson [31] proposed an equation to calculate the viscous resistance F_{vis} arising during particle movement in the liquid:

$$F_{\text{vis}} = \frac{3}{2} \frac{\pi \mu a^2}{h - x} U(x). \tag{6}$$

x is the distance that a sphere penetrates into the liquid layer; a is the sphere radius; h is the liquid layer thickness; μ is the liquid viscosity; $U(x)$ is the velocity of the sphere at a distance of x.

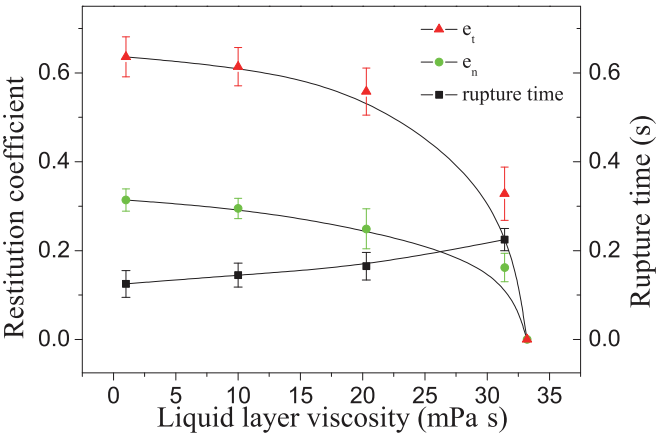

FIG. 12. (Color online) Effects of liquid viscosity on e_t, e_n, and t_{rup} (tangential velocity: 0.786 m/s; layer thickness: 2 mm).

The energy loss in the normal direction can be estimated as follows:

$$E_{\text{diss-}n} = \int_0^h \frac{3}{2}\frac{\pi\mu a^2}{h-x}U(x)dx = \mu\int_0^h \frac{3}{2}\frac{\pi a^2}{h-x}U(x)dx. \tag{7}$$

In the premise of the same layer thickness h, the integral term on the right-hand side of Eq. (7) can be considered as a constant. Thus, $E_{\text{diss-}n}$ is proportional to μ. Consequently, the increasing liquid viscosity causes larger energy dissipation that leads to a decreasing of e_n. Similarly, the drag coefficient C_D increases with the liquid viscosity, resulting in a larger drag force F_D exerting on the tangential moving sphere and a decreasing e_t.

Beside liquid bridge volume, the interfacial tension coefficient Ca also determines t_{rup}. Ca can be estimated by $\text{Ca} = \frac{\mu U}{\sigma}$ where μ is the liquid viscosity; σ is surface tension; U is the velocity of the sphere. It has been widely accepted that W_{rup} is proportional to Ca. For the present study, increasing of liquid viscosity leads to a higher Ca, which results in a larger W_{rup} and longer t_{rup}.

D. Effects of tangential impact velocity

Figure 13 provides the effects of tangential impact velocity on e_t, e_n, and t_{rup}. With the increasing of the tangential velocity, e_t decreases first and then increases, whereas e_n nearly remains unchanged and t_{rup} monotonically decays. The scatter of the data for e_t is much more prominent than that of e_n, owing to the complexity of impact in the tangential direction.

Within experimental uncertainties, the data imply that e_n is nearly independent of the tangential velocities. It further suggests that the normal and tangential velocities are essentially decoupled. The trends are the same as that observed by Kharaz *et al.* [9], Dong and Moys [32], Kantak and Davis [28], Antonyuk *et al.* [33], and Gorham and Kharaz [34]. Based on the rigid-body theory, there is a critical ratio of tangential velocity to normal velocity for a sphere obliquely impacting on a plate, below which most of the tangential kinetic energies are converted to the rotation energy (defined as "rolling region") and the dissipative kinetic energy increases, resulting in a decline of e_t. When the ratio is higher than the critical value, only a small fraction of initial kinetic energy is dissipated by the rotation (defined as "sliding region"), leading to a decrease of energy dissipation and an increase of e_t. The present results describe a transition from rolling to sliding with the increment of tangential velocity. For the present study, the critical ratio is about 0.22. Note that the critical ratio for a dry impact is around 0.57 [9], much larger than that of wet case, indicating that the coefficient of friction is drastically reduced due to lubrication effects from liquid, which significantly contributes to the reduction of critical value for the transition from rolling to sliding.

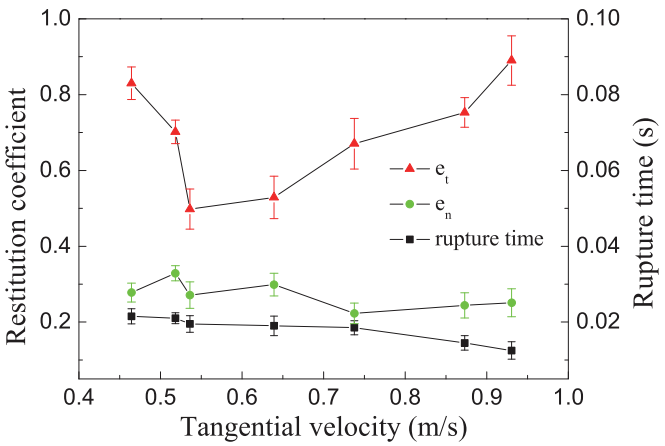

FIG. 13. (Color online) Effects of tangential velocity on e_t, e_n, and t_{rup} (liquid viscosity: 20.3 mPa s; layer thickness: 2 mm).

With the increase of tangential velocity, the mass-center velocity and angular velocity of the sphere increases so that the maximum liquid bridge force reduces [35], thereby reducing t_{rup}.

IV. DISCUSSION

A. Modified Stokes number

The previous results show that e_t and e_n strongly depend on the liquid layer thickness, liquid viscosity, and tangential velocity. In order to explore the relation between restitution coefficients and these parameters, it is reasonable to introduce a criterion in terms of dimensionless number. Normally, the dependence of restitution coefficients on the fluid and particle properties can be described by the Stokes number, St, which represents the ratio of the inertia of the sphere to the viscous forces exerted during impact on a liquid layer. The definition of St varies according to different investigated objects.

Davis *et al.* [14] proposed a definition for St (in what follows, it is referred to as "St_D"):

$$\text{St}_D = \frac{mV_i}{6\pi\mu a^2}. \tag{8}$$

St_D integrates the sphere mass m, impact velocity V_i, liquid viscosity μ, and sphere radius a, based on which, it is possible to predict whether the sphere will stick or rebound subsequent to the impact on a plate. However, St_D has its own disadvantages. It was developed to characterize the impact behavior of a sphere immersed in a viscous fluid, in which layer thickness that significantly affects the restitution coefficients is not involved. Therefore, for the impact on a liquid layer whose thickness is smaller than the sphere diameter, St_D cannot be employed to predict the rebound behavior accurately.

Gollwitzer *et al.* [36] presented a new form of St (in what follows, it is referred to as "St_G"):

$$\text{St}_G = \frac{\rho_s d V_i}{9\mu}, \tag{9}$$

where ρ_s is the density of sphere; d is the sphere diameter; V_i is the impact velocity; μ is the liquid viscosity. Similar to St_D, St_G also neglects the effects of liquid layer thickness because it is justified by $\text{Re} \ll 1$ which implies that either the liquid is highly viscous or the layer thickness is small. However, in practice, the case that spheres impact on a low-viscosity liquid layer, e.g., a water layer, is very common. Moreover, the layer thickness may be in the same order of magnitude with the sphere diameter, implying that the effects of layer thickness should not be neglected. Consequently, Eq. (9) is not appropriate for characterizing the rebound behavior of

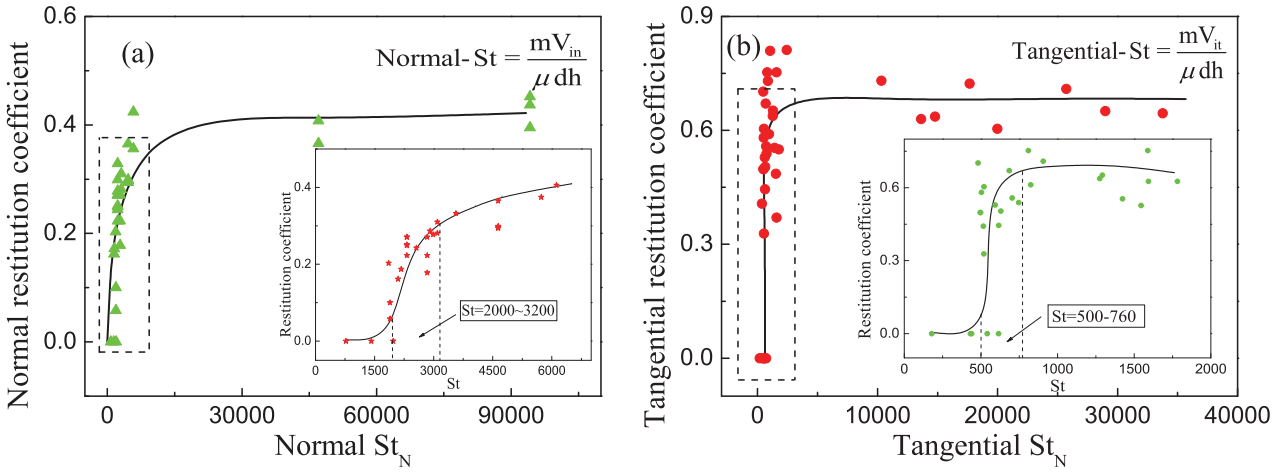

FIG. 14. (Color online) Restitution coefficients as a function of St_N.

spheres impacting on a liquid layer with various thickness and viscosities, either.

Based on the dimensional analysis, we proposed a modified Stokes number (in what follows, it is referred to as "St_N"):

$$\mathrm{St}_N = \frac{mV_i}{\mu dh}. \tag{10}$$

It is defined as the ratio of sphere initial to the viscous force and considers the effects of liquid layer thickness. m represents the sphere mass; V_i is the impact velocity; μ is the liquid viscosity; d is the sphere diameter; h is the liquid layer thickness.

Figure 14(a) shows the dependence of e_n on normal St_N (normal $\mathrm{St}_N = mV_{\mathrm{in}}/\mu dh$; V_{in} is normal impact velocity). As can be seen, a critical normal $\mathrm{St}_N \approx 2000$ (referred to as St_{Nc}) exists, below which e_n is equal to 0. It implies that a relatively low impact velocity, a highly viscous liquid, a small sphere mass, or a too-large layer thickness may all cause St_N smaller than St_{Nc}, resulting in full dissipation of kinetic energy, and no rebound occurs. Then e_n increases sharply with normal St_N in the range of 2000 and 14 000 and saturates when normal St_N is larger than 14 000. Due to the wide range of St_N, the details of the increasing process of e_n in Fig. 14(a) are not obvious. Thus, we plotted e_n versus normal St_N, covering the range from 750 to 6000 in the inset of Fig. 14(a). As normal St_N ranges from 2000 to 3200, e_n increases sharply from 0.06 to 0.31. When normal St_N exceeds 3200, e_n tends to even out.

The data were also taken to illustrate the relation between e_t and tangential St_N in Fig. 14(b). Similar to that observed for e_n, e_t also grows dramatically at small St_N and saturates at larger St_N. The corresponding critical and evening values are 500 and 1750, respectively. A significant growth of e_t from 0 to 0.675 was observed when St_N increases from 500 to 760. Then e_t fluctuates between 0.575 and 0.75 when tangential St_N ranges from 760 to 1750, followed by a saturation to 0.7 after tangential St_N exceeds 1750.

B. Energy partition analysis

In order to explore the effects of various parameters on the energy dissipation process, it is necessary to analyze the associated energy partition. During the oblique impact, the initial kinetic energy E_i is dissipated and transformed into rebound kinetic energy E_r and rotation energy E_{rot}. They can be defined as follows:

$$E_i = \tfrac{1}{2}mV_i^2, \quad E_r = \tfrac{1}{2}mV_r^2, \tag{11}$$

$$E_{\mathrm{rot}} = \tfrac{1}{2}I\omega_r^2, \tag{12}$$

where m is the sphere mass; V_i is impact velocity; V_r is rebound velocity; I is rotary inertia; ω_r is angular velocity. Figure 15 provides the plots of E_r, E_{rot}, and E_i as a function of tangential velocity. It can be seen that E_{rot} represents only a small contribution to the energy balance, implying that the majority of E_i is dissipated by the liquid phase and other dissipative processes caused by the sphere-plate contact. As the tangential velocity increases, E_r decreases first and then increases, which is similar to the variation trend of e_t with increasing tangential velocity (Fig. 13).

The total dissipated energy E_{diss} during impact can be obtained through rearranging Eqs. (2) and (3).

$$E_{\mathrm{diss}} = E_{\mathrm{diss}\text{-}n} + E_{\mathrm{diss}\text{-}t} = \left(1 - e_n^2\right)E_{\mathrm{in}} + \left(1 - e_t^2\right)E_{\mathrm{it}}. \tag{13}$$

There are two causes of the energy dissipation for the present study: dissipative processes caused by the liquid phase

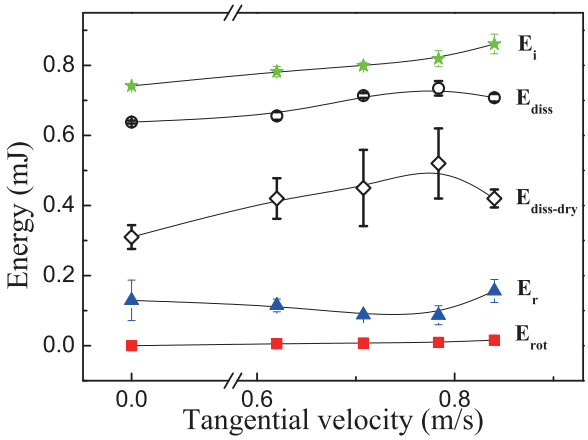

FIG. 15. (Color online) Energy partition as a function of tangential velocity (liquid viscosity: 20.3 mPa s; layer thickness: 1 mm).

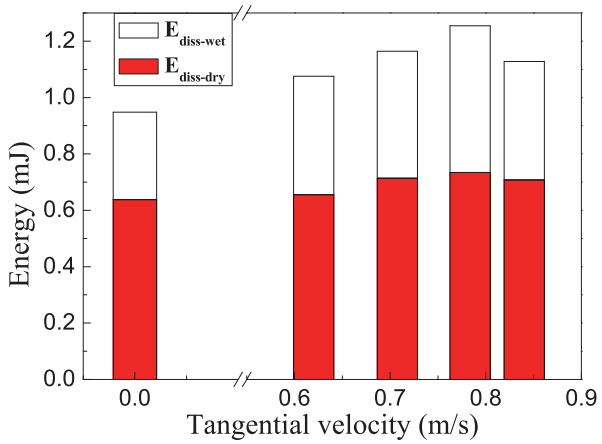

FIG. 16. (Color online) Comparison between energy loss caused by the dry and liquid phase.

(referred to as $E_{\text{diss-wet}}$); other dissipative processes caused by the sphere-plate contact, e.g., microslip, slide, deformation (referred to as $E_{\text{diss-dry}}$). Consequently, E_{diss} can be regarded as the sum of $E_{\text{diss-wet}}$ and $E_{\text{diss-dry}}$.

$E_{\text{diss-dry}}$ was estimated by Eq. (13), the required e_n and e_t of which were obtained through the experiment where spheres impact on a plate without a liquid layer. The calculated E_{diss} and $E_{\text{diss-dry}}$ as a function of tangential velocity are also plotted in Fig. 15. As can be seen, E_{diss} increases first and peaks at 0.78 m/s, then decreases with tangential velocity. A similar trend was observed when considering $E_{\text{diss-dry}}$. Note that there is considerable scatter in the data for $E_{\text{diss-dry}}$, especially for the tangential velocity ranging from 0.7 to 0.8 m/s corresponding to high $E_{\text{diss-dry}}$ values. This might be attributed to the complex mechanism of transition from rolling to sliding, in which sliding and rolling coexist. Moreover, the amount of random variation in collision geometry also leads to comparatively large scatter data.

The values of $E_{\text{diss-wet}}$ under different tangential velocities were obtained by subtracting $E_{\text{diss-dry}}$ from E_{diss}. Figure 16 plots the comparison between $E_{\text{diss-wet}}$ and $E_{\text{diss-dry}}$ under different tangential velocities. As shown, $E_{\text{diss-wet}}$ is smaller than $E_{\text{diss-dry}}$ throughout the tangential velocities investigated. $E_{\text{diss-dry}}$ mainly consists of three parts: the energy dissipated by sliding processes E_{sl}; the energy dissipated by elastic wave propagation E_{ew}; and that caused by the contact deformation E_{df}. Among them, E_{sl} and E_{ew} are comparably small. E_{df} can be estimated by tracing a sphere normally impacting on a plate without liquid layer, owing to the absence of sliding and rolling. For the present study, the values of E_{df} under various conditions are all around 0.4 mJ, which represents a significant contribution to the total energy dissipation due to elastic-plastic deformation. That coincides with the results of Antonyuk *et al.* [24] and Liu *et al.* [37]. In conclusion, the energy dissipated caused by the contact deformation and liquid phase are the two main components of the total energy dissipation.

Table I presents the proportion of energy caused by the liquid phase in the total dissipative energy. Note that the ratio decreases with the increasing of tangential velocity and reaches the minimum at 0.78 m/s, whereas $E_{\text{diss-wet}}$ almost remains unchanged, which indicates that the energy dissipation caused by the liquid phase may be independent of the tangential velocity, and the energy loss induced by the contact deformation, sliding, elastic wave propagation, etc., is the main cause of the variation in total energy dissipation.

TABLE I. Proportion of $E_{\text{diss-wet}}$ in E_{diss} under various tangential impact velocities.

Tangential velocity (m/s)	E_{diss} (mJ)	$E_{\text{diss-wet}}$ (mJ)	$E_{\text{diss-wet}}/E_{\text{diss}}$ (%)
0	0.57	0.29	51.42
0.62	0.66	0.24	35.93
0.71	0.71	0.26	36.96
0.78	0.73	0.21	29.2
0.84	0.71	0.28	40.65

V. CONCLUSION

The rebound behaviors for Al_2O_3 spheres obliquely impacting on a liquid layer were studied experimentally. The dependence of restitution coefficients on the tangential velocity and various liquid properties is discussed, associated with the Stokes number and energy dissipation analysis. Based on the investigations, the following conclusions can be drawn:

(1) Oblique impact exhibits significantly different rebound behaviors in comparison to the normal impact. Rotation occurs after oblique impact, which changes the shape of the liquid bridge formed during rebound and the corresponding liquid bridge force, finally affecting the sphere velocity.

(2) Benefiting from the lubrication effect of liquid, the angular velocity of a rebound sphere that obliquely impacts on a liquid layer is smaller than that of the dry case. For wet impact, the angular velocity increases with tangential velocity and decreases with the increasing liquid layer thickness.

(3) The increasing of liquid layer thickness and liquid viscosity may both cause declines of e_t and e_n, and increases of t_{rup}. e_t decreases first and then increases with the increasing tangential velocity, whereas e_n nearly remains unchanged and t_{rup} monotonically decays.

(4) A modified Stokes number was proposed to explore the relation between restitution coefficients (e_t and e_n) and various parameters. e_n is zero for normal $\text{St}_N \leqq \text{St}_{Nc}$, increases for normal $\text{St}_N > \text{St}_{Nc}$, and approaches an asymptotic value for normal $\text{St}_N \gg \text{St}_{Nc}$. A similar trend was observed for e_t.

(5) Concerning the energy dissipation arising during the impact, the dissipative energy caused by the contact deformation and liquid phase are the two main components of the total energy dissipation. Moreover, the energy loss caused by the liquid phase is independent of tangential velocity.

ACKNOWLEDGMENTS

Financial supports of this work by National Nature Science Foundation of China (Grants No. 51306035 and No. 51276036), and Scientific Research Foundation of the Graduate School of Southeast University are gratefully acknowledged.

[1] W. Goldsmith, *Impact* (Edward Arnold, London, 1960), p. 256.
[2] N. Maw, J. R. Barber, and J. N. Fawcett, Wear **38**, 101 (1976).
[3] K. L. Johnson, Proc. Inst. Mech. Eng. **196**, 363 (1982).
[4] C. Thornton and K. K. Yin, Powder Technol. **65**, 153 (1991).
[5] D. Tabor, Proc. R. Soc. London, Ser. A **192**, 247 (1948).
[6] D. Antypov, J. A. Elliott, and B. C. Hancock, Phys. Rev. E **84**, 021303 (2011).
[7] G. Kawabara and K. Kono, Jpn. J. Appl. Phys. **26**, 1230 (1987).
[8] N. Maw, J. R. Barber, and J. N. Fawcett, J. Lubr. Technol. **103**, 74 (1981).
[9] A. H. Kharaz, D. A. Gorham, and A. D. Salman, Powder Technol. **120**, 281 (2001).
[10] P. Mueller, S. Antonyuk, M. Stasiak, J. Tomas, and S. Heinrich, Granular Matter **13**, 455 (2011).
[11] J. Fu, M. J. Adams, G. K. Reynolds, A. D. Salman, and M. J. Hounslow, Powder Technol. **140**, 248 (2004).
[12] C. Mangwandi, Y. S. Cheong, M. J. Adams, M. J. Hounslow, and A. D. Salman, Chem. Eng. Sci. **62**, 437 (2007).
[13] J. Lundberg and H. Shen, J. Eng. Mech. **118**, 979 (1992).
[14] R. H. Davis, J. M. Serayssol, and E. J. Hinch, J. Fluid Mech. **163**, 479 (1986).
[15] P. Gondret, M. Lance, and L. Petit, Phys. Fluids **14**, 643 (2002).
[16] G. G. Joseph, R. Zenit, M. L. Hunt, and A. M. Rosenwinkel, J. Fluid Mech. **433**, 329 (2001).
[17] G. G. Joseph and M. L. Hunt, J. Fluid Mech. **510**, 71 (2004).
[18] R. Zenit and M. L. Hunt, J. Fluids Eng. **121**, 179 (1999).
[19] A. Stocchino and M. Guala, Exp. Fluids **38**, 476 (2005).
[20] G. Barnocky and R. H. Davis, Phys. Fluids **31**, 1324 (1988).
[21] M. J. Matthewson, Philos. Mag. **57**, 207 (1988).
[22] R. H. Davis, D. A. Rager, and B. T. Good, J. Fluid Mech. **468**, 107 (2002).
[23] A. A. Kantak, J. E. Galvin, D. J. Wildemuth, and R. H. Davis, Microgravity Sci. Technol. **17**, 18 (2005).
[24] S. Antonyuk, S. Heinrich, N. Deen, and H. Kuipers, Particuology **7**, 245 (2009).
[25] C. M. Donahue, W. M. Brewer, R. H. Davis, and C. M. Hrenya, J. Fluid Mech. **650**, 479 (2010).
[26] C. M. Donahue, C. M. Hrenya, and R. H. Davis, Phys. Rev. Lett. **105**, 034501 (2010).
[27] C. M. Donahue, R. H. Davis, A. A. Kantak, and C. M. Hrenya, Phys. Rev. E **86**, 021303 (2012).
[28] A. A. Kantak and R. H. Davis, J. Fluid Mech. **509**, 63 (2004).
[29] A. H. Kharaz, D. A. Gorham, and A. D. Salman, Meas. Sci. Technol. **10**, 31 (1999).
[30] R. J. Fairbrother and S. J. R. Simons, Part. Part. Syst. Charact. **15**, 16 (1998).
[31] M. J. Adams and B. Edmondson, Proc. Inst. Mech. Eng., Part J **154**, 172 (1987).
[32] H. Dong and M. H. Moys, Powder Technol. **161**, 122 (2006).
[33] S. Antonyuk, S. Heinrich, J. Tomas, N. G. Deen, M. S. van Buijtenen, and J. A. M. Kuipers, Granular Matter **12**, 15 (2010).
[34] D. A. Gorham and A. H. Kharaz, Powder Technol. **112**, 193 (2000).
[35] O. Pitois, P. Moucheront, and X. Chateau, J. Colloid Interface Sci. **231**, 26 (2000).
[36] F. Gollwitzer, I. Rehberg, C. A. Kruelle, and K. Huang, Phys. Rev. E **86**, 011303 (2012).
[37] L. X. Liu, J. D. Litster, S. M. Iveson, and B. J. Ennis, AIChE J. **46**, 529 (2000).